Wave Propagation and Granular Temperature in Fluidized Beds of Nano and FCC Particles

Michael Driscoll* **and Dimitri Gidaspow**
Department of Chemical and Environmental Engineering,
Illinois Institute of Technology,
Chicago, IL. 60616

The speeds of motion of compression waves through a fluidized bed of 10nm silica particles and 75 micron FCC particles were determined by measuring the times of arrival of compression zones using light and a gamma ray densitometer, respectively. A correlation for the modulus of elasticity for each particle type was determined as a function of void fraction. Using a kinetic theory type equation of state for particles, this experimentally determined modulus gives a value for the granular temperature for 10nm particles of approximately 1 meters per second squared. This value is close to that obtained by assuming the motion of the 10nm particles is due to collision with air molecules with no energy dissipation.

The value of the granular temperature was also determined in a two-dimensional fluidized bed by measuring the volume fraction distributions of 10nm silica particles. Granular temperatures were deduced for a one dimensional particle momentum balance using an ideal equation of state for particles, which is similar to the barometric formula for gases. These granular temperatures agreed with the measurements obtained from wave propagation experiments.

---

* Correspondence concerning this article should be addressed to Michael Driscoll at Michael.Driscoll@ge.com

Introduction

Extensive research has been performed to develop a simulation model that can predict the behavior of a fluidized gas-solid system. Sinclair (1997) presented a summary of the many different solid-gas simulation models that had been developed including a summary of a two fluid model that utilizes the solids stress modulus in the particulate momentum balance to numerically stabilize the convergence of the simulation. Knowledge of the solids stress modulus, G, is important to modeling the behavior of fluidized beds. The solids stress modulus is a thermodynamic property of a solid particle (Gidaspow, 1994) and is defined by the following equation:

$$\mathrm{G}(\varepsilon_{\mathrm{s}}) = \left(\frac{\partial \sigma_{\mathrm{s}}}{\partial \varepsilon_{\mathrm{s}}}\right)_{\mathrm{SorT}} \qquad (1)$$

Where G = Solids Stress Modulus

σ_{s} = Solids Pressure or Stress

ε_{s} =Solids Volume Fraction

Mutsers and Rietema (1977) introduced the solids stress modulus, initially called the elastic coefficient or modulus of elasticity, to explain the interparticle forces that maintain the structure of the fluidized bed during tilted bed experiments. Rietema and Piepers (1990) mathematically related the solids stress modulus to the wave propagation velocity and suggested the dependence of the solids stress modulus on the void fraction of the fluidized bed. Gidaspow (1994) provided the theoretical derivation of the solids stress modulus from mass and momentum balances in a fluidized bed. Massoundi et al. (1992), Chen and Weinstein (1992), and Gelderbloom et al (2003) reviewed the background of various correlations for the solids stress modulus. The correlations found in literature relating solids stress modulus to void fraction were either synthesized from simulation results or obtained from settling experiments. The solids stress modulus relationship actually stabilizes the simulation model by not allowing the particles to compact to unreasonably high solids volume fractions in the CFD code. Jung and Gidaspow (2002) developed a solids stress modulus correlation for Tullanox nanoparticles by inferring the solids stress gradient from the measured solids volume fraction in settling experiments assuming a solids density of 2220 kg/m^3.

Sinclair (1997) also reviewed kinetic theory models that utilize the granular temperature (a measurement of the random oscillations of particles) in the energy balance equations for a fluidized bed. The granular temperature in a fluidized bed has typically been measured by taking an average of the variance of the fluctuating velocity. Vasishta (2004) and Kalra (2005) determined the granular temperatures for three different nanoparticles in a 2D bed by solving the one dimension momentum balance and measuring the solids volume fraction in a fluidized bed. Due to the formation of porous agglomerates, the fluidization of nanoparticles has been found to occur in the dilute regime. In the dilute regime, the Particulate Ideal State Equation can be applied and the granular temperature in the riser can be determined in a relatively straightforward manner from the wave propagation velocity through a fluidized bed.

The experiments presented in this report evaluate the solids stress modulus by measuring the characteristic velocity of the one-dimensional wave through the fluidized bed. The characteristic velocity for fluidized particles is shown to be the sum of the bulk solids velocity plus the square root oscillating velocity (or the solids stress modulus divided by the solids density). Further, for dilute solids where the Particulate Ideal State

Equation ($P_s = \rho_s \varepsilon_s \theta$) applies, it will be shown that the characteristic velocity is also equal to the square root of the granular temperature. The detailed derivation of these equations follows.

Theoretical Background

The proposed experiment is based on the derivation of critical flow theory of granular materials presented by Gidaspow (1994). The derivation is initiated by stating the one-dimensional mass and momentum balances for the granular flow of solids.

Mass Balance for the Solids Phase

$$\frac{\partial(\rho_b)}{\partial t} + \frac{\partial}{\partial y}(\rho_b v_s) = 0 \qquad (2)$$

Momentum Balance for the Solid phases

$$\frac{\partial(\rho_b v_s)}{\partial t} + \frac{\partial}{\partial y}(\rho_b v_s v_s) = -\frac{\partial \sigma_s}{\partial y} + g(\rho_s - \rho_g)\varepsilon_s - \beta_B(v_s - v_g) \qquad (3)$$

Rearranging and substituting into in matrix form yields

$$\begin{pmatrix} \dfrac{\partial \rho_b}{\partial t} \\ \dfrac{\partial v_s}{\partial t} \end{pmatrix} + \begin{pmatrix} v_s, & \rho_b \\ \dfrac{G}{\rho_b} & v_s \end{pmatrix} \begin{pmatrix} \dfrac{\partial \rho_b}{\partial y} \\ \dfrac{\partial v_s}{\partial y} \end{pmatrix} = \begin{pmatrix} 0 \\ \dfrac{\varepsilon_s(\rho_s - \rho_f)g}{\rho_b} - \dfrac{\beta_B(v_s - v_g)}{\rho_b} \end{pmatrix} \qquad (4)$$

The characteristic determinant for these equations is:

$$\begin{vmatrix} v_s - \lambda & \rho_b \\ \dfrac{G'}{\rho_b} & v_s - \lambda \end{vmatrix} = 0 \qquad (5)$$

The characteristic direction for a fluidized system of particles is

$$\lambda = \frac{dx}{dt} = v_s \pm \sqrt{\frac{G}{\rho_s}} = v_s \pm \sqrt{G'} \tag{6}$$

Based on this characteristic equation for one-dimensional flow, the modified solids stress modulus, G', may be back calculated from the solids velocity and the characteristic velocity.

Now, since nanoparticles and tend to fluidize in a dilute solid volume fraction regime, the particulate ideal equation of state will apply. Therefore, by definition:

$$P_s = \rho_s \varepsilon_s \theta \tag{7}$$

The ideal particulate equation of state strictly applies for dilute systems $(\varepsilon_s \leq 0.05)$. This requirement is consistent with fluidized nanoparticle systems that typically operate at solids volume fractions under 0.03. Now, recalling.

$$G' = \frac{G}{\rho_s} = \frac{1}{\rho_s}\left(\frac{\partial P_s}{\partial \varepsilon_s}\right) \tag{8}$$

Inserting the ideal equation of state into this equation yields:

$$G' = \frac{1}{\rho_s}\left(\rho_s \theta\right) = \theta \tag{9}$$

Now, equating the characteristic velocity with this equation yields:

$$G' = \left(\frac{dx}{dt}\right)^2 = \theta \tag{10}$$

Therefore, the characteristic velocity from the shock wave experiments can be used to calculate the granular temperature and the modified solids stress modulus for the nanoparticle systems.

Experimental Equipment

The proposed experimental setup is shown in Figure 1.

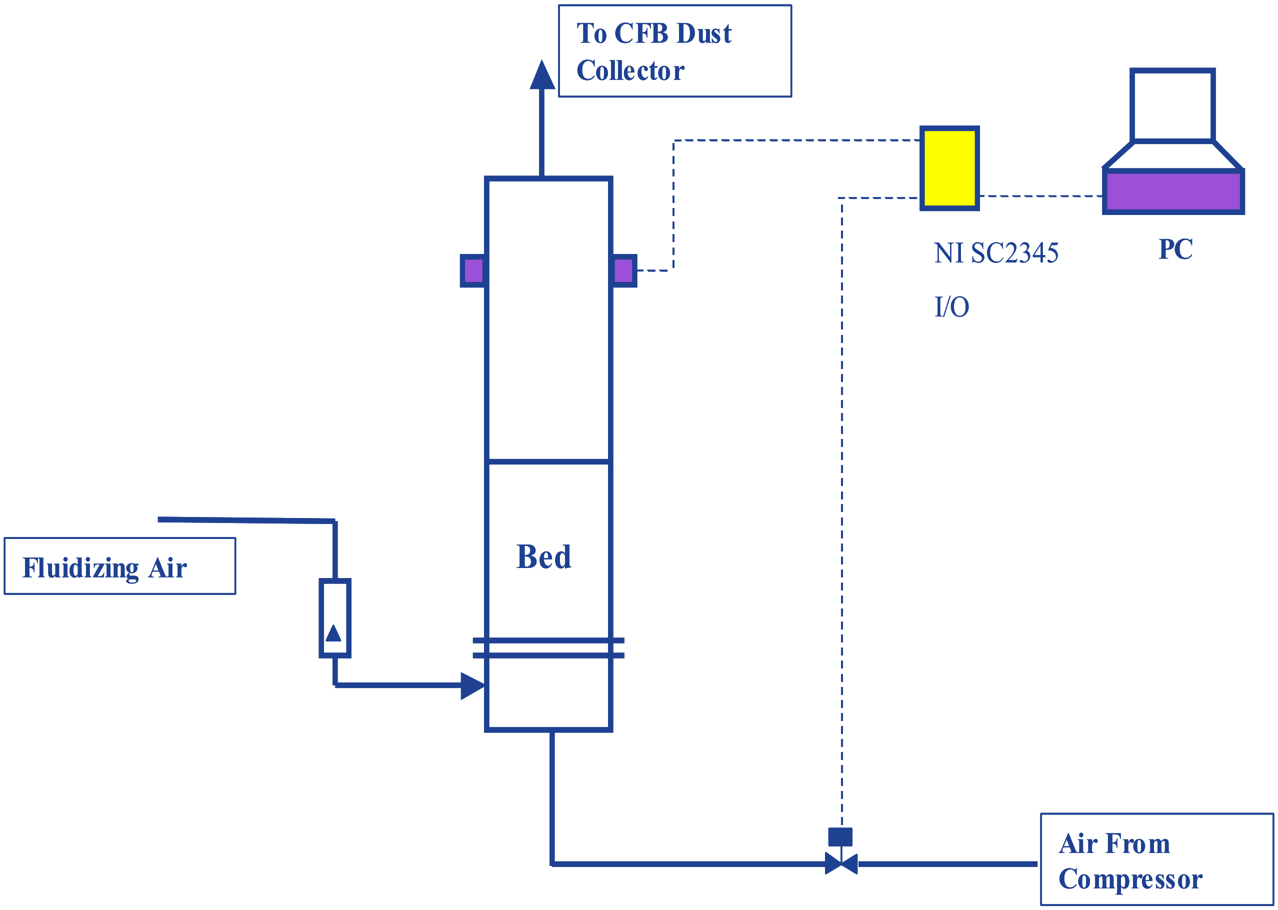

Figure 1. Schematic Diagram for Riser Experiments

The experiment was initiated by adding a specific amount of solid particles to the riser. The height of the non-fluidized bed and the weight of material added were recorded. A constant flow rate of air is then injected into the riser to fluidize the particle bed. The new fluidized height for the bed is recorded. The passage of the compression wave was detected using a gamma ray densitometer for the FCC particles and a light diode assembly for the nanoparticles. The voltage generated by the detectors is inversely proportional to the solids volume fraction of the fluidized bed. The voltage signal is collected using a National Instruments data collection system. The voltage signal is sent to a NI SCC-AI05 2 channel 100mv analog input module. This analog input module resides in a NI SC-2345 portable shielded module carrier. The NI SC-2345 is connected to a NI PCI-6221 M Series Multifunction DAQ card in a PC. The experimental data is collected every millisecond and saved into an Excel spreadsheet utilizing Labview software to direct and store the data. Next, a quick acting valve is actuated. The valve is controlled by a personal computer. The PC will be used to store the voltage data generated by the photovoltaic cell. By recording the time the valve is opened, the time required for the solids wave to travel to the sensor, the distance to the sensor, and the solids volume fraction of the bed, a correlation of G or G' versus volume fraction can be developed.

75 micron FCC Catalyst Experimental Results

A series of experiments were conducted to understand the impact of a shock wave through a fluidized bed of 75 micron FCC particles. The results of the experimental runs are summarized in Table 1.

Table 1 – FCC Particle Experimental Summary

	State	Valve to	Valve Tf	Valve Delta t	Solid Shift t	Solid Time delta	Distance (m)	Solids Velocity (m/s)
Test 1	Fluidized	4.56	5.34	0.78	7.15	2.59	3.56	1.37
Test 6	Fluidized	2.43	3.25	0.82	4.77	2.35	3.56	1.51
Test 7	Fluidized	1.57	1.98	0.41	3.32	1.75	3.56	2.03

This set of experiments measured the critical velocity through a fluidized bed containing a 75micron FCC catalyst using a gamma ray densitometer to measure the compression wave passing through the riser. Figure 2 presents the gamma ray signal as a function of time for first FCC test.

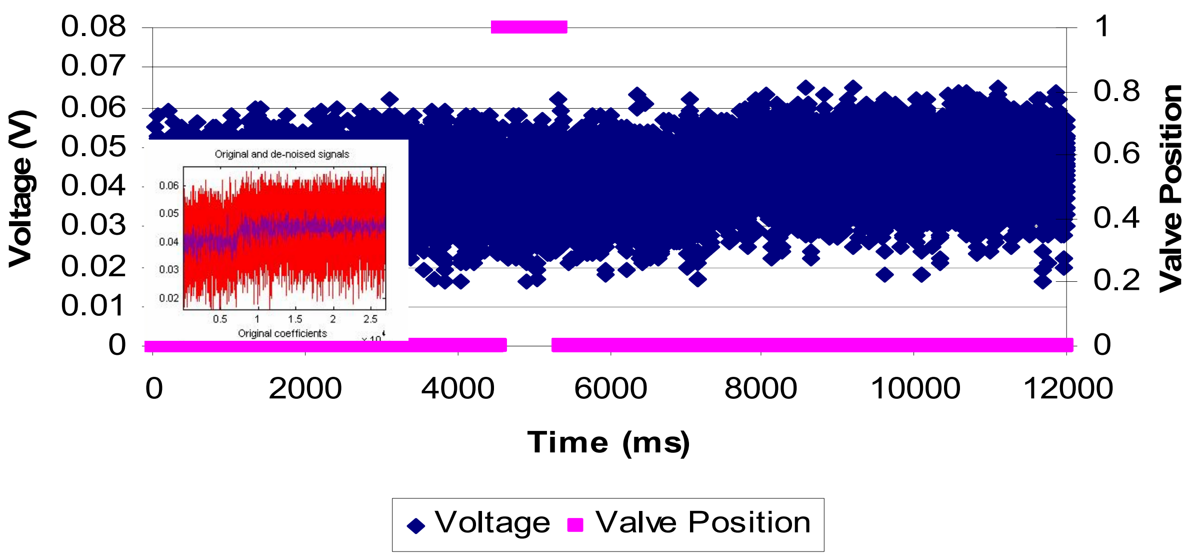

Figure 2. Voltage Signal Versus Time For First FCC Experiment

The gamma ray voltage signal runs approximately constant for the first 7000ms then shows a small dip followed by an upward shift. This graph shows the gamma ray signal drops (as the solids compression wave passes) and then increases as the particles are blown through the bed. To determine the exact point of the transition, a Haar Wavelet analysis was used to de-noise the measured data. The results of the de-noising process are presented on the insert of Figure 2. The wide signal of the insert is the raw data. The inner signal is the de-noised signal. This test showed a significant shift just after 7000ms. The second and third trials showed similar trends. This experiment yielded a critical velocity of

$$v_c = \frac{dx}{dt} \approx \frac{\Delta x}{\Delta t} = \frac{(3.56\text{m})}{(7.15 - 4.56\,\text{sec})} = 1.37\text{m/s} \tag{11}$$

Therefore, the solids stress modulus (assuming negligible solids velocity) can be calculated as follows:

$$G = \rho_s \left(\frac{dx}{dt}\right)^2 = (1400\text{kg/m}^3)(1.37\text{m/s})^2 = 2628\text{N/m}^2 \tag{12}$$

Development of Solids Stress Modulus Correlation for FCC Catalyst

The data from these experiments was analyzed statistically to understand the causal relationship between the solids stress modulus and the bed void fraction. The following relationship between solids stress modulus and void fraction for the FCC particles was determined via statistical analysis.

$$G = 10^{-14.99\varepsilon + 9.19} \tag{13}$$

Figure 3 compares this correlation to past solids stress modulus correlations.

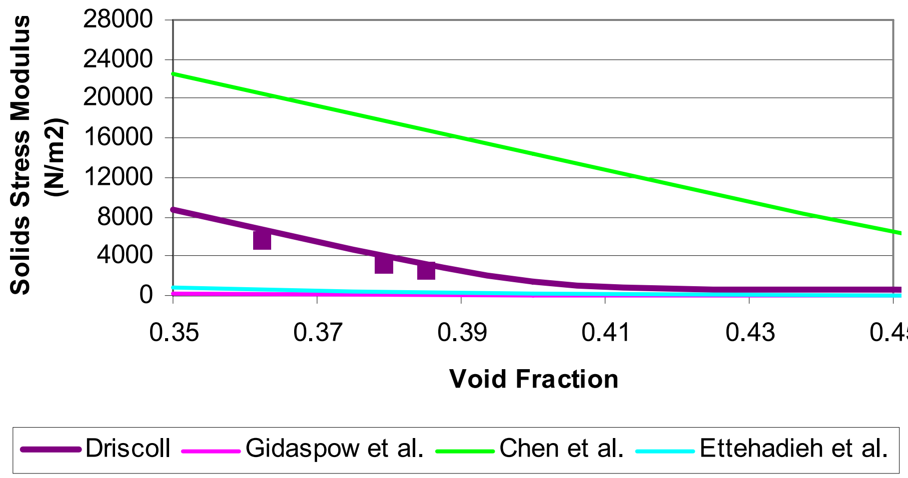

Figure 3. Comparison of Solids Stress Modulus Correlations

The new correlation compares favorably with the previous correlations presented in this graph. These graphs show a strong correlation between solids stress modulus and the void fraction over a small range of void fractions. This relationship shows the same qualitative relationship as previous correlations used in the simulation of fluidized beds.

Tullanox Nanoparticle Experimental Results

The solids volume fraction for the Tullanox nanoparticles as a function of time is compared to the SVF data for 500-micron glass beads (Seo, 1985) in Figure 4. This graph shows that that range of the solids volume fraction (SVF) for 500micron glass beads (0.45-0.7) is approximately ten times greater than the range of the SVF of the nanoparticles (0-0.02). The large range of the SVF for fluidized glass beads is due to the formation of bubbles in the fluidized bed. The tight range of the SVF for nanoparticles supports the observations that fluidization occurs without the formation of bubbles.

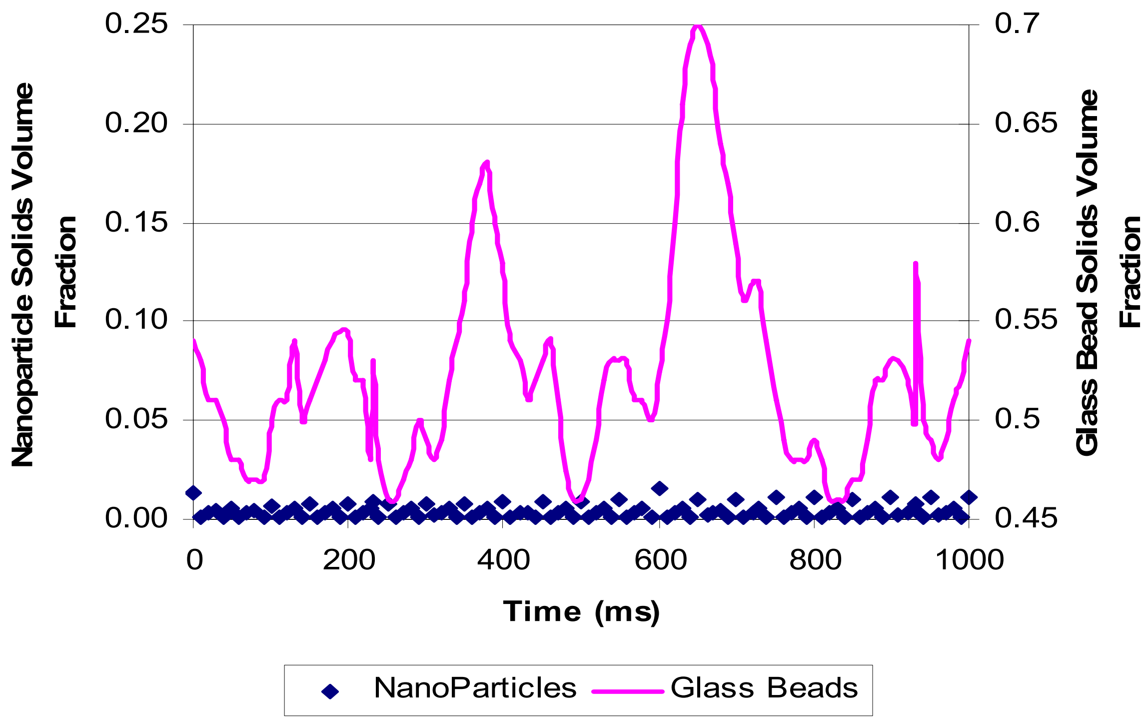

Figure 4. Solids Volume Fraction Variation For Nanoparticles and Glass Beads

Figure 5 presents the light diode voltage signal and the position of the inlet valve as a function of time for the first test. The voltage signal runs approximately constant for the first 5000ms then shows a sharp spike downward followed by an upward shift. This graph shows the voltage signal drops sharply (as the solids compression wave passes) and then increases as the particles are blown through the bed.

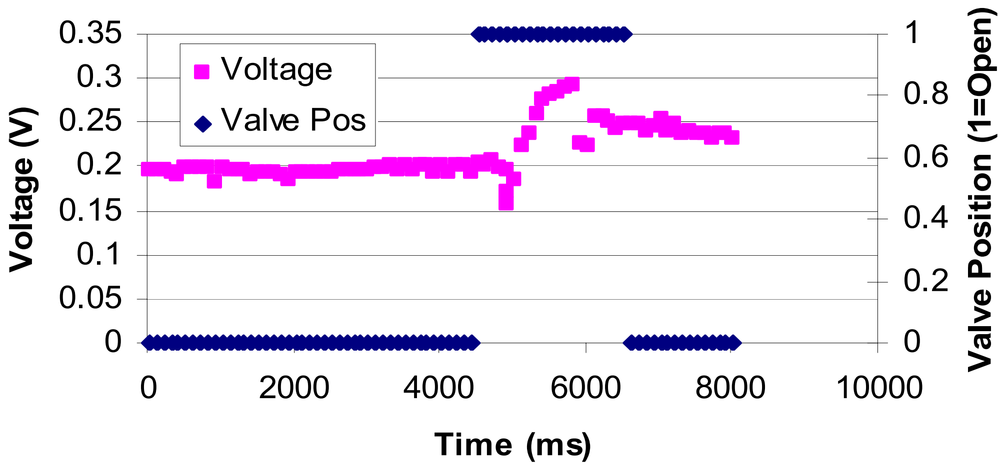

Figure 5. Voltage Signal Versus Time For First Nanoparticle Experiment

The first nanoparticle test of the experiment yielded a critical velocity of

$$v_c = \frac{dx}{dt} \approx \frac{\Delta x}{\Delta t} = \frac{(0.70\text{m})}{(4.95 - 4.46\,\text{sec})} = 1.44\text{m/s} \tag{14}$$

Therefore, the modified solids stress modulus (assuming negligible solids velocity) can be calculated as follows:

$$G' = \frac{G}{\rho_{agg}} = \left(\frac{dx}{dt}\right)^2 = (1.44\text{m/s})^2 = 2.07\text{m}^2/\text{s}^2 \tag{15}$$

The experimental results for the additional tests showed trends similar to the first test. The numerical results for these tests are summarized in Table 2.

Table 2
Experimental Results For Tullanox Nanoparticles

Bed Height (m)	H/Ho	to (sec)	tf (sec)	dt (sec)	dx (m)	vc (m/s)	G' (m2/s2)
1.46	3.41	4.46	4.95	0.49	0.70	1.44	2.07
2.17	5.05	4.63	5.20	0.57	0.70	1.24	1.55
2.15	5.02	4.39	5.01	0.63	0.70	1.13	1.27
1.09	2.53	4.48	4.88	0.40	0.70	1.77	3.12
1.12	2.62	4.56	5.00	0.45	0.70	1.58	2.51
1.50	3.51	4.92	5.45	0.53	0.70	1.33	1.77

The granular temperature can be calculated from this experimental data via the relationship presented previously (Eq.10). Figure 6 presents the granular temperature as a function of void fraction for these experiments. This graph shows a relatively flat dependence of granular temperature on void fraction.

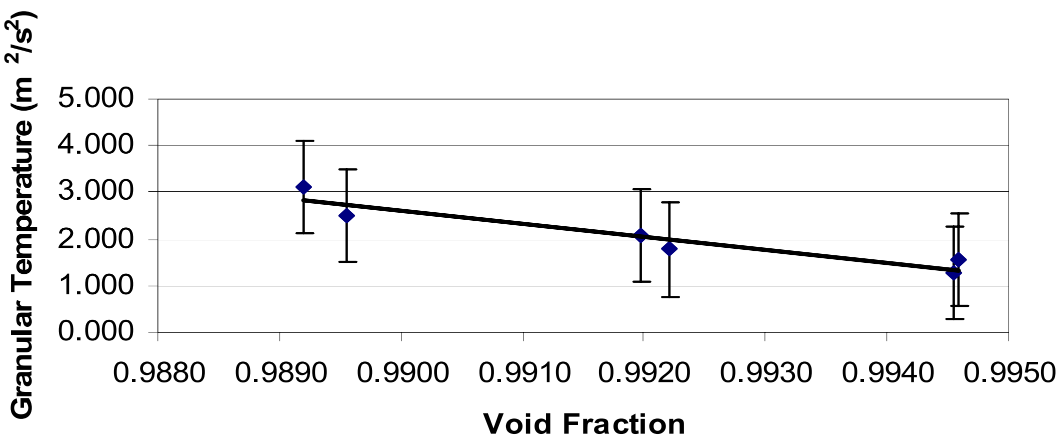

Figure 6. Granular Temperature For Nanoparticle Experiments

The value of granular temperatures measured in these experiments is consistent with the values reported in previous experiments for rectangular beds shown in Figure 7.

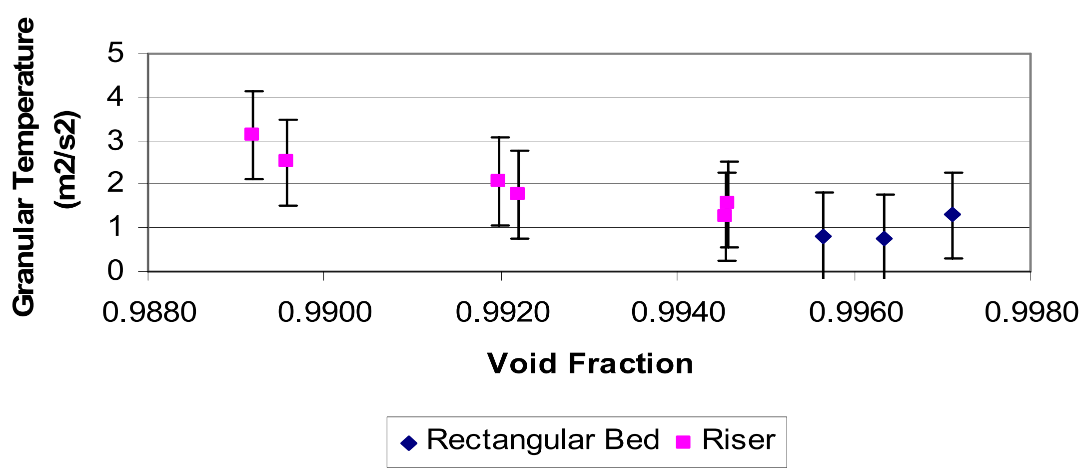

Figure 7. Granular Temperature For Riser and Rectangular Bed Experiments

These graphs show the granular temperature for Tullanox nanoagglomerates to vary to linearly with void fraction.

Modified Solids Modulus Correlation

The data from the nanoparticle experiments was analyzed statistically to understand the causal relationship between the modified solids stress modulus and the bed void fraction for nanoparticles. The following relationship between modified solids stress modulus and void fraction was determined via this analysis.

$$G' = 10^{-58.6586\varepsilon + 58.4817} \tag{16}$$

The relationship has a p-value of 0.002 and a R-Sq value of 92.1%. The correlation shows a strong causal relationship between the Log G' and the void fraction. This correlation was compared to the correlation from Jung and Gidaspow assuming an agglomerate density of 200 kg/m^3. The comparison of the two correlations is presented in Figure 8.

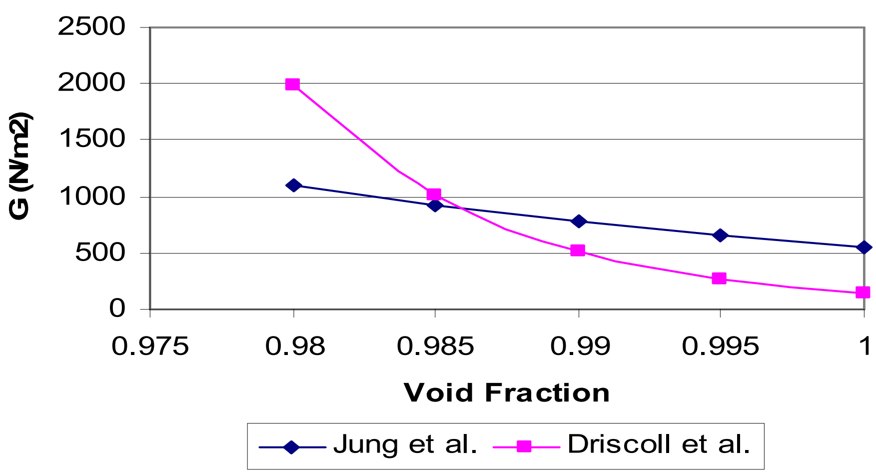

Figure 8. Comparison of Solids Stress Modulus Correlations

This graph shows a good agreement between these correlations.

Conclusions:

This study provided a novel method to experimentally develop a causal relationship between the solids stress modulus and the void fraction for FCC particles. The new correlations were consistent with past theoretical correlations and can be used to stabilize the viscosity model for simulating gas solid flow in a fluidized bed.

This study also presented a new method for finding the granular temperature and the modified solids stress modulus of a fluidized riser of nanoparticles. The granular temperature measured ranged from approximately 1 m^2/s^2 to 3 m^2/s^2.

Symbols:

β_B = Drag Coefficient

ε_s =Solids Volume Fraction

G =Solids Stress modulus

θ =Granular Temperature

σ_s = P_s = Solids Pressure

ρ_s = Solids density

v= velocity

Acknowledgement

The authors would like to acknowledge the contributions of Mr. Mayank Kashyap during the execution of the experimental runs. Mayank provided dedicated help in the collection of the data for the experiments presented in this report.

References

Chen, L., and H. Weinstein, "Measurement of Normal Stress and Hinderance Factor in a Collapsing Bed," Chem. Eng. Sci., **49(**6), 811 (1994).

Fan, L.S. and Chao Zhu, Principles of Gas-Solid Flows, Cambridge University Press, Cambridge, New York (1997).

Gelderbloom, S.J., Gidaspow, D., and R.W. Lyczkowski, "CFD Simulations of Bubbling/Collapsing Fluidized Beds for Three Geldart Groups," AIChE J., **49**, 844(2003).

Gidaspow, D., Multiphase Flow and Fluidization: Continuum and Kinetic Theory Descriptions, Academic Press, New York (1994).

Gidaspow, D., and R. Mostofi, "Maximum Carrying Capacity and Granular Temperature of A, B, and C Particles," AIChE J., **49(**4), 831(2003).

Huang, C., Wang, Y., and Fei Wei, "Multi-stage Agglomerate Structure and Solids Mixing Behavior of Nano-particle in Fluidized Bed," AIChE Spring Meeting Conference Proceedings, **2**, 248c (2006).

Jung, J., Design and Understanding of Turbulent, Bubbling and Slurry Column Reactors, PhD Thesis, Illinois Institute of Technology, Chicago (2003).

Jung, J. and D. Gidaspow, "Fluidization of nano-size particles," Journal of Nanoparticle Research, **4**, 483(2002).

Kalra, J., Fluidization of Silica Nano-Size Particles in Circulating and Two Dimensional Fluidized Beds, Masters Thesis, Illinois Institute of Technology, Chicago (2005).

Kunii, D., and D. Levenspiel, Fluidization Engineering, 2nd Ed. Butterworth-Heinemann, Boston(1991).

Kwauk, M., and J. Li, "Fluidization regimes," Powder Technology, **87**, 193(1996).

Kwauk, M., Li, J., and D.Liu, "Review Particulate and aggregative fluidization – 50 years in retrospect," Powder Technology, **111**, 3(2000).

Li, H., Hong, R., and Z. Wang, "Fluidizing ultrafine powders with circulating fluidized bed," Chem. Eng. Sci., **54**, 5609(1999).

Li, H., Lu, X., and M. Kwauk, " Particulatization of gas-solids fluidization," Powder Technology, **137**, 54(2003).

Massoudi, M., K.R. Rajagopal, J.M. Ekmann, and M.P. Mathur, “Remarks on the Modeling of Fluidized Systems,” AIChE J., **38**, 47(1992).

Mutsers, S.M.P., and K. Rietema, “The Effect of Interparticle Forces on the Expansion of a Homogeneous Gas-Fluidized Bed,” Powder Technology, **18**, 239(1977).

Rietema, K., and H.W. Piepers, “The Effect of Interparticle Forces on the Stability of Gas-Fluidized Beds – I. Experimental Evidence,” Chem. Eng. Sci., **45**(6), 1627(1990).

Roy, R., Davidson, J.F., and V.G. Tuponogov, “The Velocity of Sound in Fluidised Beds,” Chem. Eng. Sci., **45**(11), 3233(1990).

Seo, Y., Fluidization of Single and Binary Size Particles, Ph.D. Thesis, Illinois Institute of Technology, Chicago, Illinois(1985).

Sinclair, J.L., “Hydrodynamic Modeling,” Circulating Fluidized Beds, Blackie Academic and Professionals, **149**(1997).

Vasishta, V., Kalra, J., Singh, R., Jung, J., and D. Gidaspow, Fluidization of Nano-particles in the IIT Riser, Illinois Institute of Technology, Chicago, 2003.

Vasishta, V., Hydrodynamics of Fluidization and Settling of Silica Nanoparticles, Masters Thesis, Illinois Institute of Technology, Chicago(2004).

Wang, Y., Gu, G., Wei, F., and J. Wu, “Fluidization and Agglomerate Structure of SiO_2 Nanoparticles,” Powder Technology, **124**, 152(2002).

Wang, Y., Wei, F., Jin, Y., and T. Luo, “Bed Collapse Behavior of Primary Nanoparticles,” Fluidization X edited by Kwauk, M., J. Li and W.C. Wang, New York, 477(2001).

Wang, Z., Kwauk, M., and H. Li, “Fluidization of Fine Particles,” Chem. Eng. Sci., **53**, 377(1998).

Yang, W., “Fluidization of Fine Cohesive Powders and Nanoparticles – A Review ,“ J. Chin. Inst. Chem. Engrs., **36**(1), 1(2005).

Yao, W., Guangsheng, G., Fei, W., and W. Jun, “Fluidization and agglomerate structure of SiO_2 Nanoparticles,” Powder Technology, **124**, 152(2002).

Zhu, C., Yu, Q., Dave, R., and R. Pfeffer, ”Gas Fluidization Characteristics of Nanoparticle Agglomerates,” AIChE J., **51**(2), 426(2005).